Entropy residual shock detector for shock-capturing using high-order discontinuous Galerkin scheme

By Y. Lv AND M. Ihme

1. Motivation and objectives

The lack of robustness, especially for under-resolved flow features, is one of the major barriers impeding the application of high-order numerical schemes to technical problems. Flow-field discontinuities, such as shocks and contacts, are typical examples of such under-resolved flow features. Without any treatment, high-order approximations of these discontinuities result in unbounded oscillations (often referred to as non-linear instabilities (Dumbser *et al.* 2014)) that lead to the divergence of the solver. Because of this deficiency, the development of shock-stabilization techniques have gained substantial attention in recent years. However, the accurate detection of discontinuities is an essential requirement for effectively applying these shock-stabilization techniques. Without a robust shock detector, the solution in smooth flow regions might be improperly modified, resulting in deterioration in the numerical accuracy and the physical description. Hence, there has been a strong push to develop a robust shock detector for localizing discontinuous solutions. In this regard, the development of shock detection has been widely addressed in the context of finite-volume and finite-difference schemes. Jameson *et al.* (1981) proposed using the cell-wise pressure jump as a shock sensor for finite volume schemes, widely used for supersonic aerodynamic flow calculations. For high-order reconstruction-based finite volume schemes, the relative difference between the reconstructed face value and the cell-centered value for pressure or density is proven to be very robust for localizing shocks even in complex flow configurations (Khalighi *et al.* 2011; Nichols *et al.* 2012). Ducros *et al.* (1999) extended Jameson's shock detector to finite-difference schemes, and combined it with the relative magnitude between dilatation and vorticity for application to shock/turbulence interaction problems. Later, Bhagatwala & Lele (2009) extended the idea by Ducros *et al.* to consider the dilatation in the vicinity of shocks. Sjögreen & Yee (2004) proposed a wavelet shock detector that determines the discontinuity by referring to the Lipschitz exponent of a characteristic variable expanded on a chosen non-orthogonal wavelet basis. Ziegler *et al.* (2011) developed a shock detector for hybrid WENO-central finite difference schemes based on Liu's entropy condition that localizes shocks if the characteristic speed is locally bounded by the values on the left and right sides of the stencil.

For high-order discontinuous Galerkin (DG) schemes, several shock detectors have been proposed. An earlier version of the shock detector is embedded in the TVB(total variation bounded) limiter with a tunable parameter (Cockburn & Shu 1989). This detector has been adopted primarily in DGP1 and DGP2 schemes, and the results have been shown to be insensitive to this value over a relatively broad range of conditions. Krivodonova *et al.* (2004) proposed a shock detector that is based on the jump of density or entropy at element interfaces. This detector shows good performance in most of the tests but might

result in some mis-detection along shear layers. Vuik & Ryan (2014) developed a detection procedure by projecting the DG-solution onto a multiwavelet basis. Troubled cells are then identified if there is a noticeable growth in high-level modes in the multiwavelet decomposition are noticeable. To compare the performance of different detectors, the reader is referred to the review by Qiu & Shu (2005). Essential requirements on a shock detector are: 1) capability to distinguish smooth and discontinuous parts of the solution, 2) adaptability to different problem settings and a wide range of operating conditions, and 3) extendability to arbitrary discretization schemes and spatial dimensions.

With these in mind, one objective here is to develop a shock detector that is based on an entropy residual. For generic conservation laws, the entropy residual is zero where the solution is sufficiently regularized, and strictly negative in the region with non-smooth and discontinuous solutions (Lax 1971; Tadmor 1986). Physically, the entropy residual plays an essential role in distinguishing discontinuities from smooth solutions. This property naturally fulfills the first requirement listed above, with which we intend to explore the potential of using the entropy residual as a novel shock detector for high-order numerical schemes on general grids and a wide range of flow conditions. Similar to other detectors, a flagging criterion for troubled cells takes the form of

$$|\widetilde{R}_{\mathcal{U}}(U_e)| > \varepsilon \,, \tag{1.1}$$

where the left-hand side (LHS) is the detection function that is built on the entropy-residual $\widetilde{R}_{\mathcal{U}}$ and ε is a threshold value. An attractive property of this method, demonstrated in this work, is that the detection function converges to zero for smooth solutions, so that the shock stabilization is strictly applied only to non-smooth and under-resolved regions in the flow field. In addition, a dynamic threshold-setting (DTS) procedure is proposed to automatically determine ε by considering shocks with different characteristics.

The remainder of the report is organized as follows: Section 2 introduces the governing equations, the discretization scheme and the artificial-viscosity formulation. The formulation and consistent discretization of the entropy residual is introduced in Section 3. This is followed by analyzing the convergence property, which represents the essential part of this work. To supplement this shock-detection approach, a detailed discussion on setting the threshold will be given in Section 4. Section 6 is concerned with application of the detector to a number of test cases, including several supersonic problems with different discontinuities, shock-vortex interaction, and detonation configurations. A comparison with different shock detectors is included. The manuscript finishes with our conclusions.

2. Mathematical model and numerical techniques

2.1. *Governing equations*

The governing equations that are the basis of the current work are a system of conservation laws, written as

$$\partial_t \mathsf{U} + \nabla \cdot \mathsf{F} = 0 \,, \tag{2.1}$$

where the solution variable $\mathsf{U} \in \mathbb{R}^{N_v}$ and the convective flux term $\mathsf{F} \in \mathbb{R}^{N_v \times N_d}$. Here, N_v is the dimension of the solution vector, and N_d denotes the spatial dimensionality. The temporal derivative is denoted by ∂_t, and ∂_i represents the derivative with respect to the spatial dimension x_i. This system has an associated entropy extension. For a convex

function $\mathcal{U} = \mathcal{U}(\mathsf{U})$, we have the relation Tadmor (1986)

$$\partial_t \mathcal{U} + \nabla \cdot \mathcal{F} \leq 0 \,, \tag{2.2}$$

where $\mathcal{F}$ is the corresponding entropy flux. In the region of a smooth solution, the equality holds, while the LHS becomes negative in the vicinity of discontinuous solutions. To regularize the system at discontinuities, a Laplacian viscosity term is added to the right-hand side (RHS) of Eq. (2.1)

$$\mathsf{D} = \nabla \cdot \mathsf{F}_{\mathrm{AV}} = \nabla \cdot (\mu_e \nabla \mathsf{U}) \,, \tag{2.3}$$

with μ_e being the artificial viscosity. Since we consider a variational formulation, we assume that μ_e is an element-wise constant in this study.

2.2. *DG discretization*

We consider the problem to be posed in the domain Ω with boundary $\partial\Omega$. A mesh partition is defined as $\Omega = \cup_{e=1}^{N_e} \Omega_e$, where Ω_e corresponds to a discrete element of this partition. The edge of element Ω_e is defined as $\partial\Omega_e$. To distinguish different sides of the edge, the superscripts $+$ and $-$ are used, denoting the interior and exterior, respectively. We define a global space of test functions as

$$\mathcal{V} = \oplus_{e=1}^{N_e} \mathcal{V}_e \;\; \text{with} \;\; \mathcal{V}_e = \mathrm{span}\{\varphi_n(\Omega_e)\}_{n=1}^{N_p} \,, \tag{2.4}$$

where φ_n is the nth polynomial basis, and N_p is the number of bases. On the space $\mathcal{V}_e$ we seek an approximate solution to Eq. (2.1) of the form

$$\mathsf{U} \simeq U = \oplus_{e=1}^{N_e} U_e \,, \qquad U_e \in \mathcal{V}_e \,, \tag{2.5}$$

where the solution vector U_e in each individual element takes the general form

$$U_e(t,x) = \sum_{m=1}^{N_p} \widetilde{U}_{e,m}(t) \varphi_m(x) \,. \tag{2.6}$$

The unknown vector of the basic coefficients $\widetilde{U}_{e,m} \in \mathbb{R}^{N_v \times N_p}$ is obtained as the solution to the discretized variational form of Eq. (2.1) with the addition of the artificial viscosity

$$\frac{d\widetilde{U}_{e,m}}{dt} \int_{\Omega_e} \varphi_n \varphi_m d\Omega - \int_{\Omega_e} \nabla \varphi_n \cdot F(U_e) d\Omega + \int_{\partial\Omega_e} \varphi_n^+ \widehat{F}(U_e^+, U_e^-, \vec{\mathrm{n}}) d\Gamma = D(U_e, \varphi_n) \,, \tag{2.7}$$

$\forall \varphi_n$ with $n = 1, \ldots, N_p$. The numerical Riemann flux $\widehat{F}$ is evaluated based on the states at both sides of the interface $\partial\Omega_e$ and the outward-pointing normal vector $\vec{\mathrm{n}}$. In this study, we use the Rusanov flux (Rusanov 1961) to compute $\widehat{F}$.

The RHS of Eq. (2.7), $D(U_e, \varphi_n)$, is the discretized diffusion term for shock stabilization. The detailed mathematical form of this term has been presented in our previous report (Lv & Ihme 2014). The numerical discretization of this term is carried out using the BR2 scheme (Bassi & Rebay 2000), because of compactness-preserving and optimal convergence properties. Time integration is facilitated by a Runge-Kutta scheme, leading to a RKDG framework, originally developed by Cockburn & Shu (1989, 1998). This framework was further extended (Lv & Ihme 2015) to enhance the robustness by imposing entropy boundedness. This treatment avoids the appearance of nonphysical quantities. Because of this significant advantage, all algorithms in the present study are implemented in this entropy-bounded discontinuous Galerkin (EBDG) solver.

3. Development of a shock detector based on entropy residual

In this section, we will introduce the concept of entropy residual and its discretization. This is followed by numerical analysis of the fully discretized form of the entropy residual.

3.1. *Entropy residual*

For a generic system of conservation laws with entropy extension, the entropy residual of an entropy function, $\mathcal{U}(\mathsf{U})$, is defined as

$$R_{\mathcal{U}} = \partial_t \mathcal{U} + \nabla \cdot \mathcal{F} \,, \tag{3.1}$$

for the exact solution (Tadmor 1986; Guermond & Pasquetti 2008). To facilitate shock detection, we construct a measure for the entropy residual of the discretized solution. For this, we represent the exact solution in Eq. (3.1) with the cell-local approximation, U_e, and evaluate the element-wise entropy residual by the following semi-discrete form

$$R_{\mathcal{U}}(U_e) = \frac{1}{|\Omega_e|} \int_{\Omega_e} \left[\partial_t \mathcal{U}(U_e) + \nabla \cdot \mathcal{F}(U_e)\right] d\Omega \,. \tag{3.2}$$

Since U_e is a local approximation to U_e, the property of the true entropy residual is expected to be retained in this formulation, subject to approximation errors. The temporal derivative is approximated by a finite difference scheme,

$$\widetilde{R}_{\mathcal{U}}(U_e) = \frac{1}{|\Omega_e|} \int_{\Omega_e} \left[\frac{\mathcal{U}(U_e(t+\Delta t)) - \mathcal{U}(U_e(t))}{\Delta t} + \frac{1}{2}\nabla \cdot (\mathcal{F}(U_e(t)) + \mathcal{F}(U_e(t+\Delta t))\right] d\Omega \,, \tag{3.3}$$

which produces the fully discretized approximation to the element-wise entropy residual. Here, we propose only one way to discretize the entropy residual, but other methods, such as variational discretization, are equally possible. However, as we are using Eq. (3.3) as a detector, we found that Eq. (3.3) introduces the least computational overhead and provides a straightforward and intuitive implementation.

3.2. *Numerical analysis*

To conduct numerical analysis, the necessary notations and preliminaries are first introduced. We use $||\cdot||_{\mathrm{r}}$ to denote the Sobolev norm in H^{r}, where H is a Hilbert space. When $\mathrm{r} = 0$, it reduces to the standard L^2-norm. In addition, we use the notation $\mathcal{P}^{\mathrm{p}}$ to denote a polynomial space of order p. We also recall the following theorem (Babuška & Suri 1987), which forms the foundation for our analysis.

THEOREM 1. *For $X \in H^r(\Omega_e)$ and its polynomial approximation $X^h \in \mathcal{P}^p(\Omega_e)$, we have*

$$||X - X^h||_{q,\Omega_e} \leq C h_e^{\sigma-q} ||X||_{r,\Omega_e} \,,$$

for $0 \leq q \leq \sigma$, and $\sigma = \min(p+1, r)$, where h_e is the size of the element Ω_e and C is a constant that is independent of X and h_e.

According to this theorem, if X is sufficiently smooth, for instance, $X \in H^\infty$, we can expect optimal convergence for the approximation error in L^2:

$$||X - X^h||_{0,\Omega_e} \leq C_1 h_e^{p+1} \,,$$
$$||\partial_i X - \partial_i X^h||_{0,\Omega_e} \leq C_2 h_e^{p} \,.$$

For convenience, here we embedded $||X||$ into the constants C_1 and C_2, although it is not essential to the analysis.

By utilizing these results, an error estimate for the proposed detection function can be established. Consider an approximation to a sufficiently regularized solution that satisfies $R_{\mathcal{U}}(\mathsf{U}) = 0$. Upon applying RKDG, there is strong evidence (Cockburn & Shu 1989, 1998) that the optimal convergence can be achieved in the L^2-norm under a proper CFL (Courant-Friedrichs-Lewy) constraint. In other words, for $t \in [t^n, t^n + \Delta t]$,

$$||\mathsf{U} - U||_{0,\Omega} \leq C_3 h_m^{\mathrm{p}+1} \ , \tag{3.4}$$

where $h_m = \max_e\{h_e\}$ and C_3 might depend on U, t or p, but is independent of h_m (the same is true for the constants introduced next). According to Theorem 1, this observation implies that the exact solution U is at least in $H^{\mathrm{p}+1}$. Furthermore, with the relation $||\mathsf{U} - U||^2 = \sum_e ||\mathsf{U}_e - U_e||^2$, we can also obtain an error estimate for a cell-local solution in Ω_e, taking the form

$$||\mathsf{U}_e - U_e||_{0,\Omega_e} \leq C_3 h_m^{\mathrm{p}+1} \ . \tag{3.5}$$

We can also conclude that

$$||\nabla \cdot \mathsf{U}_e - \nabla \cdot U_e||_{0,\Omega_e} \leq \sum_i ||\partial_i \mathsf{U}_e - \partial_i U_e||_{0,\Omega_e} \leq C_4 h_m^{\mathrm{p}} \ . \tag{3.6}$$

The next step is to derive the error estimate for the entropy function and the flux terms. This estimate generally requires that both $\mathcal{U}$ and $\mathcal{F}$ are at least H^1 functions of U, so that

$$||\mathcal{U}(\mathsf{U}_e) - \mathcal{U}(U_e)||_{0,\Omega_e} \lesssim \sup_{\Omega_e} \left|\partial \mathcal{U}/\partial \mathsf{U}\right| \ ||\mathsf{U}_e - U_e||_{0,\Omega_e} \leq C_5 h_m^{\mathrm{p}+1} \ , \tag{3.7}$$

$$||\nabla \cdot \mathcal{F}(\mathsf{U}_e) - \nabla \cdot \mathcal{F}(U_e)||_{0,\Omega_e} \lesssim \sup_{\Omega_e} |\partial \mathcal{F}/\partial \mathsf{U}| \ ||\nabla \cdot \mathsf{U}_e - \nabla \cdot U_e||_{0,\Omega_e} \leq C_6 h_m^{\mathrm{p}} \ , \tag{3.8}$$

where the absolute-valued operator $|\cdot|$ is applied to each entry of the vector. Under the desired CFL-constraint, the established error estimates, Eqs. (3.5)-(3.8), hold over the entire time interval $[t^n,\ t^n + \Delta t]$. With these relations and the Cauchy-Schwarz inequality, the manipulation leads to the following relation:

$$\Delta t |\Omega_e| |\widetilde{R}_{\mathcal{U}}(U_e)| \leq C_7 |\Omega_e|^{1/2} h_m^{\mathrm{p}+1} + C_8 |\Omega_e| \Delta t^2 + C_9 |\Omega_e|^{1/2} \Delta t h_m^{\mathrm{p}} \ . \tag{3.9}$$

By introducing the relation $|\Omega_e| \sim h_m^{N_d}$ and a generic CFL-constraint $\Delta t \sim \ h_m$ for convection-dominated problems, we obtain

$$|\widetilde{R}_{\mathcal{U}}| \leq C_{10} h_m^{\mathrm{r}}, \qquad \mathrm{r} = \min\left(\mathrm{p} - \frac{N_d}{2}, 1\right) \ . \tag{3.10}$$

Hence, for a high-order approximation ($\mathrm{p} \geq 2$ with at least third-order accuracy) to smooth problems, the detection function introduced here, $|\widetilde{R}_{\mathcal{U}}|$, has first-order convergence with respect to grid refinement under the condition $\mathrm{p} \geq 1 + N_d/2$. The numerical property has important implications: Suppose that troubled cells are initially flagged due to poor resolution. With increasing resolution (i.e., p or h refinement) the magnitude of the detection function decreases, and after the resolution reaches a certain level such that $|\widetilde{R}_{\mathcal{U}}|$ becomes lower than the threshold ε, no troubled cells will be flagged. This numerical property will be verified through test cases in Section 6.

4. Dynamic threshold setting (DTS)

In the previous section, numerical properties of the proposed entropy-residual formulation were analyzed for sufficiently smooth solutions. For non-smooth solutions, the entropy-residual detection function is expected to be of order unity. Based on this significant magnitude difference, a threshold value ε is commonly set in the detection criterion, Eq. (1.1). However, based on our experience, this direct approach often fails due to its insensitivity to shock discontinuities with different characteristics. For example, if gas-dynamic applications are of concern, it is easy to imagine that the threshold designated for hypersonic flows has to be different from that for a weak shock with a Mach number slightly above one. Therefore, from a practical point of view, we have to incorporate sensitivity into our detection criterion so that it is adaptable to the local solution with different characteristics.

Now the question arises over the magnitude of the detection function in the presence of a shock discontinuity. To determine this, we attempt to estimate a local upper bound by using the element-averaged information in the troubled cell and its compact neighbors. In the following, an element-averaged quantity is denoted by an overbar, and the maximum value among its compact neighborhood is denoted by a star. For demonstration purposes, we consider the Euler system, and we assume that the total change in entropy in Ω_e is small over Δt. For a numerically diffused shock front inside or around Ω_e, the detection function can be approximated as

$$
\begin{aligned}
|\widetilde{R}_{\mathcal{U}}| &\sim \frac{1}{|\Omega_e|}\int_{\Omega_e}\frac{\partial(\rho u s)}{\partial x_1}d\Omega_e\,, && \text{(assume the maximum of entropy flux variation along } x_1\text{)}\\
&\sim \frac{1}{h_e}(\bar{\rho}^*\bar{u}^*\bar{s}^* - \bar{\rho}\bar{u}\bar{s})\,, && \text{(approximate sub-cell using neighboring information)}\\
&\sim \frac{\bar{s}}{h_e}(\bar{\rho}^*\bar{u}^* - \bar{\rho}\bar{u})\,, && (\bar{s}^* = \bar{s} + \mathcal{O}(\Delta u^3))\\
&\sim \frac{\bar{s}\bar{\rho}v_s}{h_e}\left(\frac{\bar{\rho}^*}{\bar{\rho}} - 1\right)\,, && \text{(introduce } v_s \text{ as shock velocity)}\\
&\sim \underbrace{\frac{1}{h_e}\left(|\bar{u}| + \bar{c}\sqrt{\frac{\gamma-1}{2\gamma} + \frac{\gamma+1}{2\gamma}\frac{\bar{p}^*}{\bar{p}}}\right)\frac{\frac{2}{\gamma-1}\left(\frac{\bar{p}^*}{\bar{p}} - 1\right)\bar{s}\bar{\rho}}{\frac{\gamma+1}{\gamma-1} + \frac{\bar{p}^*}{\bar{p}}}}_{C_{11}^e}\,. && \text{(shock jump relation)}
\end{aligned}
$$

According to this analysis, the magnitude of the detection function is confirmed to be of order unity in the presence of shock discontinuities due to the CFL-constraint $\Delta t \sim h$. Meanwhile, the introduced parameter C_{11}^e contains the influence of the local flow characteristics on the entropy residual, in the presence of a local pressure ratio, $\bar{p}^*/\bar{p}$. Based on this estimate, we conservatively propose $\varepsilon = C_{11}^e$ as a local threshold in Ω_e, which is one order of magnitude smaller than the estimated value and incorporates the local solution's characteristics. In addition, by comparing this result with Eq. (3.10), we can expect this threshold to be effective in avoiding misdetection of smooth solutions, since it is generally one order of magnitude larger than the resulting detection function. In the above estimate, $\bar{p}^*/\bar{p}$, applies under the assumption of the existence of a shock discontinuity. If this ratio is lower than the pressure ratio resulting from a shock, for consistency with the assumption, we replace $\bar{p}^*/\bar{p}$ in the above formulation with the

pressure ratio across a weak shock. In closing note, this shock detector has been developed independently of any specific shock-stabilization technique.

5. Reference detectors for comparative study

The entropy-residual detector that we developed is compared to the shock detectors proposed by Krivodonova *et al.* (2004) and by Persson & Peraire (2006). For the former, troubled cells are flagged based on the solution jump along elemental interfaces

$$I_e = \frac{|\int_{\partial\Omega_e}(\Phi_e - \Phi_{nb_e})d\Gamma|}{h^{(\mathrm{p}+1)/2}|\partial\Omega_e|||\Phi_e||} , \tag{5.1}$$

where Φ is a scalar quantity, often chosen to be density or entropy (Krivodonova *et al.* 2004). According to the original paper, for the condition that

$$I_e > 1 \tag{5.2}$$

is satisfied, Ω_e is determined as a troubled cell. As for the work by Persson & Peraire (2006), the smoothness of local solution is quantified as

$$S_e = \frac{\int_{\Omega_e}\left(\Phi_e - \Phi_e^{\mathrm{p}-1}\right)^2 d\Omega}{\int_{\Omega_e}\Phi_e^2 d\Omega} , \tag{5.3}$$

in which Φ is also a scalar quantity and $\Phi_e^{\mathrm{p}-1}$ refers to the representation on a truncated basis with order $\mathrm{p}-1$. According to the Fourier expansion, the quantity S_e is proportional to p^{-4} for smooth profiles. For a non-smooth solution, S_e becomes large and deviates from this scaling arguments. Therefore, a criterion adapted from Persson & Peraire (2006) can be proposed as

$$S_e > c_{\mathrm{pp}}\mathrm{p}^{-4} \tag{5.4}$$

for selecting troubled cells, where c_{pp} is a tunable parameter and depends on flow configurations and scheme resolutions. Since the purpose of this paper is not to optimize the performance of the shock detector, we selected a relatively optimal value for c_{pp} through a posterior assessment. Furthermore, Φ is chosen to be the physical entropy. Although entropy is attributed to all the shock detection procedures considered here, for the shock detectors by Krivodonova *et al.* (2004) and by Persson & Peraire (2006) the entropy is used as a scalar field. In our approach, entropy is only part of the contribution from the entropy-residual evaluation of Eq. (3.3). The developed DTS procedure is also applied for our entropy-residual detector.

6. Numerical test cases

For the following numerical test cases, we consider the set of Euler equations, Eqs. (2.1), with

$$\mathsf{U} = (\rho,\ \rho u,\ \rho e)^T , \tag{6.1a}$$

$$\mathsf{F} = (\rho u,\ \rho u \otimes u + \boldsymbol{I}p, u(\rho e + p))^T , \tag{6.1b}$$

in which ρ, u, p and e refer, respectively, to density, velocity, pressure and specific total energy. The closure for this system is the ideal gas law

$$p = (\gamma - 1)\rho\left(e - \frac{|u|^2}{2}\right) , \tag{6.2}$$

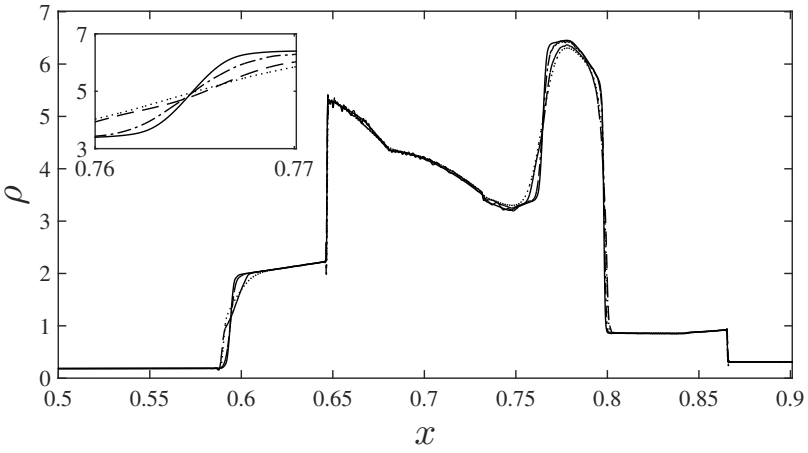

FIGURE 1. Prediction of the blast wave problem using three different shock detectors with $h = 1/800$ and p = 4 at $t = 0.038$ (Exact−solid line; entropy-residual detector−dashed line; Krivodonova et al.'s detector (Krivodonova *et al.* 2004)−dotted line; detector adapted from Persson & Peraire (2006) with $c_{\text{pp}} = 0.01$−dotted dashed line).

and γ, the ratio of specific heat capacities, is set to a constant value of 1.4. We use the physical entropy to define the entropy variable and entropy flux, so that

$$\mathcal{U} = -\rho s \,, \tag{6.3}$$

$$\mathcal{F} = -\rho u s \,, \tag{6.4}$$

where $s = \ln(p) - \gamma \ln(\rho) + s^0$. The CFL-numbers for the following simulations are taken from Table 1 of Lv & Ihme (2015).

6.1. *Blast wave problem*

This case is considered to examine the performance in the presence of extremely strong shocks. The initial conditions are defined as

$$(\rho, u, p)^T = \begin{cases} (1, 0, 1000)^T & \text{for } x \leq 0.1 \,, \\ (1, 0, 0.01)^T & \text{for } x > 0.1 \text{ and } x \leq 0.9 \,, \\ (1, 0, 100)^T & \text{for } x > 0.9 \,, \end{cases} \tag{6.5}$$

on a one-dimensional domain with $x \in [0, 1]$. The simulation runs until $t = 0.038$. The reference solution is obtained using WENO5 with 12000 finite-volume cells. The performance of the entropy-residual shock detector is illustrated in Figure 1 with comparison to the performance of the other two detectors. Compared to Krivodonova et al.'s detector (Krivodonova *et al.* 2004), the entropy-residual detector avoids the selection of troubled elements inside expansion waves. Furthermore, the entropy-residual detector tends to be slightly more aggressive than the Persson and Peraire's detector (Persson & Peraire 2006) in selecting troubled elements along the shock fronts. In this comparison, the main advantage of the entropy-residual detector is that it is parameter-free and does not require the user's intervention. For this specific problem, we found that the left contact front is sensitive to numerical dissipation and requires substantial numerical resolution. The detector adapted from Persson & Peraire (2006), which introduce the least dissipation, provides the closest solution to the reference solution around there.

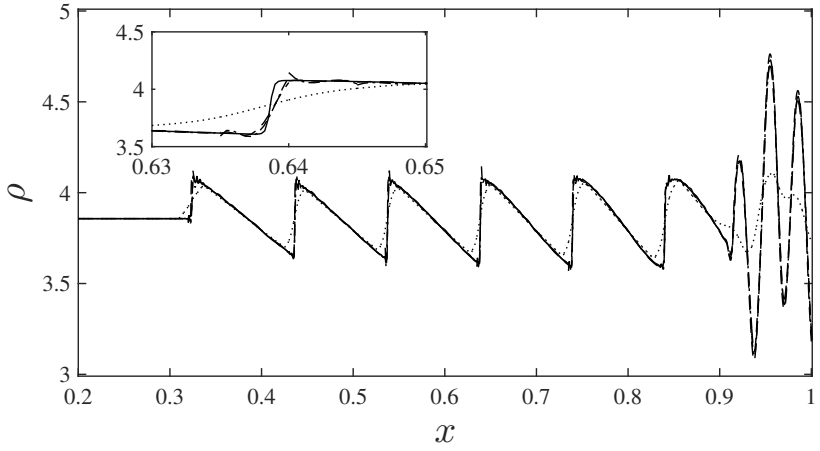

FIGURE 2. Prediction of Shu-Osher problem using three different shock detectors with $h = 1/200$ and p = 4 at $t = 0.30$ (Exact−solid line; entropy-residual detector−dashed line; Krivodonova et al.'s detector (Krivodonova *et al.* 2004)−dotted line; detector adapted from Persson & Peraire (2006) with $c_{\text{pp}} = 0.01$−dotted dashed line).

6.2. *Shu-Osher problem*

This test aims at examining the performance of the shock-capturing scheme in the presence of high-frequency density waves. The setup was originally proposed by Shu & Osher (1989). The initial conditions are defined as

$$(\rho, u, p)^T = \begin{cases} (3.8571, 2.6294, 10.3333)^T & \text{for } x \leq 0.125\ , \\ (1.0 + 0.2\sin(50x), 0.0, 1.0)^T & \text{for } x > 0.125\ , \end{cases} \tag{6.6}$$

on a one-dimensional domain with $x \in [0, 1]$. The simulation runs until $t = 0.18$ according to the original case setting (Shu & Osher 1989). The reference solution is obtained using WENO5 with 12000 finite-volume cells. The performance of the entropy-residual shock detector is assessed and compared to the two competing shock detectors. To challenge the shock-detection procedure, we extend the simulation time to $t = 0.30$, allowing the spontaneous formation of several shock fronts at $0.3 < x < 0.9$. The characteristics on selecting troubled elements around the shock front is consistent to those observed in the above two cases. Both the entropy-residual detector and Krivodonova et al.'s detector (Krivodonova *et al.* 2004) capture the forming shocks, but the latter introduces much more numerical dissipation at high-frequency density waves, as we can see in Figure 2 (at $x > 0.9$). The shock detector adapted from Persson & Peraire (2006) with the optimal c_{pp} value yields performance comparable to that of the entropy-residual detector in selecting the troubled element. However, as shown in Figure 2, a smaller c_{pp} value is anticipated in order to remove the Gibbs phenomenon in the vicinity of forming shocks.

7. Conclusions

An entropy-residual approach was proposed for shock detection with application to high-order DG schemes. The entropy residual was introduced in a fully discretized setting and was numerically analyzed. It was shown that for smooth solutions, the detection function converges to zero. This property guarantees the deactivation of the shock sta-

bilization for smooth solutions. A dynamic threshold-setting procedure was proposed by estimating an upper bound of the entropy-residual magnitude according to cell-averaged information from local and compact neighbors. In a one-dimensional test, the proposed shock detector shows a performance superior to that of the existing shock-detection approaches, without the user's intervention.

Acknowledgments

This work was supported by an Early Career Faculty grant from NASA's Space Technology Research Grants Program. Calculations were performed on the Pleiades supercomputer at NASA.

REFERENCES

Babuška, L. & Suri, M. 1987 The optimal convergence rate of the p-version of the finite element method. *SIAM J. Numer. Anal.* **24**, 750–776.

Bassi, F. & Rebay, S. 2000 GMRES discontinuous Galerkin solution of the compressible Navier-Stokes equations. In *Discontinuous Galerkin Methods: Theory, Computation and Applications*, ed. B. Cockburn & C.-W. Shu, pp. 197–208. Berlin: Springer.

Bhagatwala, A. & Lele, S. 2009 A modified artificial viscosity approach for compressible turbulence simulations. *J. Comp. Phys.* **228**, 4965–4969.

Cockburn, B. & Shu, C.-W. 1989 TVB Runge-Kutta local projection discontinuous Galerkin finite element method for conservation laws III: one-dimensional systems. *J. Comp. Phys.* **84**, 90–113.

Cockburn, B. & Shu, C.-W. 1998 The Runge-Kutta discontinuous Galerkin method for conservation laws V: multidimensional systems. *J. Comp. Phys.* **141**, 199–224.

Ducros, F., Ferrand, V., Nicoud, F., Weber, C., Darracq, D., Gacherieu, C. & Poinsot, T. 1999 Large-eddy simulation of the shock/turbulence interaction. *J. Comp. Phys.* **152**, 517–549.

Dumbser, M., Zanotti, O., Loubere, R. & Diot, S. 2014 A posteriori subcell limiting of the discontinuous Galerkin finite element method for hyperbolic conservation laws. *J. Comp. Phys.* **278**, 47–75.

Gamezo, V. N., Desbords, D. & Oran, E. S. 1999 Two-dimensional reactive flow dynamics in cellular detonation. *Shock Waves* **9**, 11–17.

Guermond, J.-L. & Pasquetti, R. 2008 Entropy-based nonlinear viscosity for Fourier approximations of conservation laws. *C. R. Acad. Sci. Paris, Ser. I* **346**, 801–806.

Jameson, A., Schimdt, W. & Turkel, E. 1981 Numerical solutions of the Euler equations by finite volume methods using Runge-Kutta time-stepping schemes. In *AIAA 14th Fluid and Plasma Dynamic Conference*.

Khalighi, Y., Nichols, J. W., Lele, S., Ham, F. & Moin, P. 2011 Unstructured large eddy simulation for prediction of noise issued from turbulent jets in various configurations. *AIAA Paper* 2011-2886.

Krivodonova, L., Xin, J., Remacle, J.-F., Chevaugeon, N. & Flaherty, J. E. 2004 Shock detection and limiting with discontinuous Galerkin methods for hyperbolic conservation laws. *Appl. Numer. Math.* **48**, 323–338.

Lax, P. D. 1971 Shock waves and entropy. In *Contributions to Nonlinear Functional Analysis* (ed. E. H. Zarantonello), pp. 603–634. Academic Press, New York, London.

Lv, Y. & Ihme, M. 2014 Taming nonlinear instability for discontinuous Galerkin scheme with artificial viscosity. *Annual Research Briefs,* Center for Turbulence Research, Stanford University, pp. 109–122.

Lv, Y. & Ihme, M. 2015 Entropy-bounded discontinuous Galerkin scheme for Euler equations. *J. Comp. Phys.* **295**, 715–739.

Nichols, J. W., Lele, S. K., Moin, P., Ham, F. E. & Bridges, J. E. 2012 Large-eddy simulation for supersonic rectangular jet noise prediction: effects of chevrons. *AIAA Paper* 2012-2212.

Persson, P.-O. & Peraire, J. 2006 Sub-cell shock capturing for discontinuous Galerkin methods. *AIAA Paper* 2006-112.

Qiu, J. & Shu, C.-W. 2005 A comparison of troubled-cell indicators for Runge-Kutta discontinuous Galerkin methods using weighted essentially nonoscillatory limiters. *SIAM J. Sci. Comput.* **27**, 995–1013.

Rusanov, V. V. 1961 Calculation of intersection of non-steady shock waves with obstacles. *J. Comp. Math. Phys. USSR* **1**, 267–279.

Shu, C.-W. & Osher, S. 1989 Efficient implementation of essentially non-oscillatory shock-capturing schemes II. *J. Comp. Phys.* **83**, 32–78.

Sjögreen, B. & Yee, H. C. 2004 Multiresolution wavelet based adaptive numerical dissipation control for high order methods. *J. Sci. Comput.* **20**, 211–255.

Tadmor, E. 1986 A minimum entropy principle in the gas dynamics equations. *Appl. Numer. Math.* **2**, 211–219.

Vuik, M. J. & Ryan, J. K. 2014 Multiwavelet troubled-cell indicator for discontinuity detection of discontinuous Galerkin schemes. *J. Comp. Phys.* **270**, 138–160.

Ziegler, J., Deiterding, R., Shepherd, J. E. & Pullin, D. I. 2011 An adaptive high-order hybrid scheme for compressive, viscous flows with detailed chemistry. *J. Comp. Phys.* **230**, 7598–7630.